CONF-800232--1

LA-UR 80-723

TITLE: TIME INDEPENDENT MEAN-FIELD THEORY

MASTER

AUTHOR(S): J. W. Negele, T-9

SUBMITTED TO: Proceedings of the International Conference
on Extreme States in Nuclear Systems
Dresden, DOR
February 4-8, 1980

University of California

LOS ALAMOS SCIENTIFIC LABORATORY
Post Office Box 1663 Los Alamos, New Mexico 87545
An Affirmative Action/Equal Opportunity Employer

Form No. 836 R3
St. No. 2629
12/78

UNITED STATES
DEPARTMENT OF ENERGY
CONTRACT W-7405-ENG. 36

TIME DEPENDENT MEAN-FIELD THEORY

J. W. Negele
Center for Theoretical Physics, Massachusetts Institute of Technology,
Cambridge MA 02139 USA
and Los Alamos Scientific Laboratory, Los Alamos, NM 87545 USA

Abstract

The physical and theoretical motivations for the time-dependent mean-field theory are presented and the successes and limitations of the time-dependent Hartree-Fock initial value problem are reviewed. New theoretical developments are described in the treatment of two-body correlations and the formulation of a quantum mean-field theory of large-amplitude collective motion and tunneling decay. Finally, the mean-field theory is used to obtain new insights into the phenomenon of pion condensation in finite nuclei.

1. Motivation

The objective of nuclear many-body theory is to understand the observable properties of nuclear systems in terms of the underlying nucleon-nucleon interaction. Until our present qualitative ideas about the interactions between bags of quarks[1] are replaced by a tractable quantitative theory of strong interactions, nuclear theory will necessarily remain phenomenological at the level of the nucleon-nucleon interaction. However, given the nucleon-nucleon scattering data and deuteron bound state data embedded in present phenomenological potentials, it is quite reasonable to expect that the static potential approximation will not be catastrophically in error. The analogous system of liquid He, which in terms of the product of the repulsive core volume time specific density is eight times denser than nuclear matter, is particularly encouraging in this respect. Although the electron wave functions of one He atom are essentially always significantly overlapping those of at least one other atom, nevertheless a static potential may be defined conceptually clearly in terms of the Born-Oppenheimer approximation, and phenomenological static potentials determined from experimental scattering data and virial coefficients reproduce the bulk properties of liquid He quite satisfactorily

The goal of this talk, then, will be to attempt to understand the exceedingly complicated properties of composite systems bound by a two-body static potential solely in terms of that potential. Thus, we want phenomena to emerge naturally from the theory without being embedded *a fortiori* by ansatz. By this criterion, it will be illegitimate to look at a host of experimental data, note that it all seems to be described in terms of

ping those of at least one other atom, nevertheless a static potential may be defined conceptually clearly in terms of the Born-Oppenheimer approximation, and phenomenological static potentials determined from experimental scattering data and virial coefficients reproduce the bulk properties of liquid He quite satisfactorily.

The goal of this talk, then, will be to attempt to understand the exceedingly complicated properties of composite systems bound by a two-body static potential solely in terms of that potential. Thus, we want phenomena to emerge naturally from the theory without being embedded a fortiori by ansatz. By this criterion, it will be illegitimate to look at a host of experimental data, note that it all seems to be described in terms of a few selected collective variables, and then construct a theory containing only those variables. Similarly we rule out describing a class of phenomena which appear statistical empirically in terms of a theory which is only allowed to contain Gaussian distributed quantities. Rather, we seek a theory in which the initial conditions relevant to an experiment and the two-body force determine the relevant collective variables or statistical behavior. The theory itself should seek out the right shapes for intrinsic states and for vibrations, and it should generate the appropriate soft or unstable spin-isospin modes as a result of the one-pion exchange component of the force. The theory is then free of any prescription for such quantities as one or two-center shell model potentials or mass parameters, and to the degree to which it succeeds in describing nuclear systems under normal experimental conditions, it offers genuine predictive power to deal with the extreme conditions which are the topic of this conference.

The problem I have posed of understanding the properties of systems processing large numbers of degrees of freedom in terms of the underlying Lagrangian or Hamiltonian pervades all of theoretical physics, and we will thus draw heavily from many-body techniques

developed in field theory, plasma physics, solid state physics, and condensed matter physics. My approach will be to attempt to formulate a systematic hierarchy of successive approximations such that the lowest order contains the physics of the mean field. Furthermore, I will always seek to approximate the expectation values of few-body operators rather than calculate the full many-body wave function, since even in the most favorable cases in which a few body operator is well approximated by these techniques, the overlap between the exact and approximate many-body wave functions decreases exponentially in the number of particles. Physically, since the many-body wave function involves the simultaneous correlations of all N particles in the system, it is obvious that such detailed information could never be reliably embedded in a low-order approximation. For the expectation value of a finite-range few-body operator, however, the correlations of all the particles outside the range of the operator are clearly irrelevant, so there is far greater reason to hope to develop a viable approximation for such expectation values.

In addition to the aesthetic appeal of the resulting theory, there are a number of physical motivations for the choice of the mean field theory as a starting point for nuclear dynamics. One of the best justifications is Hartree's original intuitive argument that an individual particle should respond to the average field generated by interactions with the surrounding particles. For systems of the size of observed nuclei, the mean field approximation is a far more sensible starting point than the opposite extreme of assuming complete local equilibration. Instead of the mean free path generally cited by adherents of the hydrodynamical model, it seems to me that the relevant length scale for collisions is in fact the longitudinal momentum equilibration length--the distance it takes for two colliding fluids to slow down to thermal velocities. On the average, several collisions are required for thermalization, and when the nucleon-nucleon amplitudes are forward peaked, the longitudinal equilibration length is significantly longer than generally quoted values for mean free paths.[2] Since nuclear shapes evolve by motion of the surface, it is particularly important that the surface itself be treated realistically. In contrast to Thomas Fermi or hydrodynamical theories, the mean-field approximation includes the wave function phase coherence characteristic of the nuclear surface

so that the kinetic energy density and thus evolution of the surface should be specified reasonably reliably. Finally, because of the proliferation of misconceptions, it is useful to emphasize the fact that the mean-field theory includes a great deal of the physics of two-body collisions. The mean field, of course, is completely generated by the two-body potential. Furthermore, all forward scattering amplitudes and one-particle one-hole amplitudes defined with respect to this instantaneous one-body density matrix are included, and only the two-particle two-hole amplitudes are neglected.

Given the ambitions of this program, it is clear that a very high price must be paid in the numerical complexity of the resulting equations. In many cases, the problem may be rendered tractable, or nearly so, by the introduction of physically motivated approximations. The most crucial of these is to assume that the short range correlations in the time-dependent problem differ negligibly from those in nuclear matter, and thus to use directly effective interactions derived from nuclear matter, or equivalently, simple Skyrme-like parametrizations of these effective interactions.[3] The status of nuclear matter theory and effective interactions is well documented in this literature[4-6] and will not be discussed further. Additional reductions in computational effort may be effected by the imposition of various symmetries.[5,7,8]

As a final motivation for the time-dependent mean-field theory, it is useful to survey briefly some salient results for stationary states and small vibrations built upon these states and to note the quantitative agreement with experimental charge distributions which is attained. Figure 1 shows the rather spectacular agreement of theoretical

predictions for elastic electron scattering from ^{208}Pb with the subsequent experimental data from Saclay.[9] Comparison of the theoretical density with the charge distribution reconstructed from the data in Fig. 2 shows the quantitative precision obtained in the nuclear surface, with the only significant discrepancy being the tendency of the mean-field approximation to exaggerate shell fluctuations. In this case, the central maximum arises from the complete occupation of the 3s proton state, and should be somewhat reduced by configuration admixtures produced by the residual interaction.[10] Having verified adequate treatment of the nuclear surface, the next essential test is that the mean field reproduce the correct shapes of deformed intrinsic states. One observes from the mean-field predictions for the shapes of a variety of rare-earth and actinide nuclei in Fig. 3 that the theory specifies far more about quadrupole, hexadecapole and higher multipole deformations than a single deformation parameter, and it is indeed gratifying that the $0^+ \rightarrow L^+$ form factors shown in Fig. 4, which essentially determine the Fourier transform of the L^{th} component of a Legendre expansion of the density, agree with experiment to almost the same precision as in the elastic form factor of ^{208}Pb. In the vibrational model, one obtains a test of various derivatives of the intrinsic density distribution, and Fig. 5 demonstrates again the validity of the mean field theory of the ^{238}U intrinsic state.[12] Finally, since the familiar random phase approximation (RPA) is just the infinitesimal amplitude limit of the time-dependent mean-field theory discussed below, in Fig. 6, we have shown how well the collective 3^- state in Pb is reproduced in the mean field approximation.

II. Theory

Insight into the theoretical content and possible systematic generalizations of the time-dependent mean-field theory is obtained by considering alternative formulations of the time-dependent Hartree Fock (TDHF) initial value problem. (One should note that there is a tendency in the literature to sloppily interchange the term Hartree Fock, which implies use of the bare two-body interaction, with the term mean-field, which refers to either a bare or effective interaction. In theoretical derivations, it is clear whether a bare or effective interaction is intended in principle, and for realistic calculations, an effective interaction is always used.)

2.1 The TDHF Initial Value Problem

It is convenient to express the TDHF equations in terms of the one-body density matrix, in which case the equation of motion is

$$i\dot{\rho} = [h,\rho] \tag{1}$$

where

$$\rho(x,x',t) \equiv \langle \psi^{+}(x',t)\ \psi(x,t) \rangle \tag{2}$$

and

$$h \equiv K + \mathrm{tr}\ \rho v \tag{3}$$

$$\equiv K + \int dx_2 dx_4 \langle x_1 x_2 | v | x_3 x_4 - x_4 x_3 \rangle\ \rho(x_4, x_2)$$

Since the equation is first order in time, the density matrix at any subsequent time is fully determined by specifying a one-body density matrix at the initial time. If the initial density matrix corresponds to a determinant, i.e. satisfies $\rho^2 = \rho$, it will continue to do so at all later times, but eq. (1) is not necessarily restricted to determinants. The TDHF equation, eq. (1), is applied to the scattering of nuclei semi-classically by localizing the initial positions of the centers of static HF solutions for the target and projectile and boosting these Galilean invariant HF solutions to the desired incident cm velocities.

Postponing, for the moment, the conceptual ambiguities of this semiclassical treatment of scattering, two computational results are shown in Figs. 7 and 8 which demonstrate that eq. (1) quantitatively reproduces the strong dissipation observed in low energy heavy ion phenomenology. Since the fusion cross section requires slowing down the projectile enough to form a compound nucleus for a range of impact parameters forming a disk (or annulus!) of impact parameters of the proper area, the data in Fig. 7 are a very sensitive diagnostic of dissipation.[14] Similarly, in the deep inelastic collision[15] shown in Fig. 8, the crucial issue is whether the mean field generates enough excitation energy in the final fragments so that in the deep inelastic peak and backward directions, they recede with essentially only the Coulomb barrier energy and no residual translational collective energy. With two enticing examples suggesting that the time-dependent mean-field theory may retain some of the quantitative predictive power already demonstrated by the static mean field theory, we now turn to several alternative derivations.

2.2 Alternative Formulations

Perhaps the most economical way to obtain eq. (1) is application of the time-dependent variational principle.[16]

Varying the action

$$\delta \langle \Psi | i \frac{\partial}{\partial t} - H | \Psi \rangle \tag{4}$$

with no restriction on the form of Ψ simply yields the many-body Schrodinger equation

$$i \frac{\partial}{\partial t} | \Psi \rangle = H | \Psi \rangle \tag{5}$$

Restricting Ψ to be a Slater determinant

$$\Psi = \sum_{p} (-)^{p} \phi_{i}(x_{pi}) \tag{6}$$

yields the following set of equations equivalent to eq. (1)

$$i\dot{\phi}_{i} = h\phi_{i} \tag{7}$$

where h is defined in eq. (3). Explicit formulation of the theory in terms of a many-body wave function has the obvious advantage that we have a familiar language in which to think about the theory and to relate to alternative approximations. Thus, one observes that at each instant, the TDHF wave function acquires exactly the correct one-particle one-hole components and differs from the state produced by evolution with the full Schrodinger equation precisely by neglecting all two-particle two-hole components. One also can appreciate how significantly the TDHF wave function differs in general from the lowest state in the adiabatic instantaneous basis generated by h by simply expanding the TDHF wave function in that basis. One disadvantage of this forumlation in terms of a wave

also can appreciate how significantly the TDHF wave function differs in general from the lowest state in the adiabatic instantaneous basis generated by h by simply expanding the TDHF wave function in that basis. One disadvantage of this forumlation in terms of a wave function is the obvious temptation to take more than its one-body density matrix seriously. A second disadvantage is the fact that it is not obvious how to implement a sequence of systematic improvements in the variational ansatz.

An alternative derivation of eq. (1) is to truncate the Martin-Schwinger Green's function hierarchy.[17] In general the time derivative of G_N is related to G_{N+1}, G_N, and G_{N-1} and the equation of motion for G_1 is

$$[i \frac{\partial}{\partial t_1} - T(x_1)]G_1(1,1') = \delta(1,1') - i\int dx_2 v(x_1-x_2)\, G_2(1,2;1',2^+)\Big|_{t_2=t_1} \qquad (8)$$

Making the obvious approximation that the two-particle Green's function is the anti-symmetrized product of two single-particle Green's functions

$$G_2(1,2;1'2') \cong G_1(1\,1')G_1(2\,2') - G_1(1\,2')G_1(1'2)$$

again yields the TDHF approximation.[5] Adoption of corresponding prescriptions for G_3 in terms of G_2 and G_1 thus offers the possibility of obtaining a closed equation for the two-body correlations contained in G_2. Although such formal developments have been carried out by Orland and Schaeffer[18] and by Tang[19], the full theory is so cumbersome that it has not yet been applied to any problems, and implementable approximations to the full theory are laden with dubious prescriptions.

Yet another formulation is based on truncation of the time-dependent coupled-cluster hierarchy[20], the time independent limit of which has successfully been applied to stationary states of nuclei with realistic interactions.[21] The many body wave function is

written

$$|\Psi\rangle = e^{S_1+S_2+\ldots+S_n}\,|\phi\rangle \equiv e^{S}|\phi\rangle \qquad (9)$$

where $|\phi\rangle$ denotes a States determinant and S_m represents a general sum of m particle--m hole amplitudes. Multiplying the Schrodinger equation by e^{-S} and projecting onto a complete set of states

$$\langle\phi|\, a^{+}_{\nu_1} \ldots a^{+}_{\nu_m} a_{\rho_m} \ldots a_{\rho_1}\, e^{-S}\{H - i\frac{\partial}{\partial t}\}\, e^{S}|\phi\rangle = 0 \qquad (10)$$

and expanding the multicommutator series yields a set of coupled equations in which $\dot{S}_m$ is a functional of S_{m+2} and lower S's. The TDHF approximation is recovered by setting $S_m=0$ for all $m \geq 2$, and higher approximations are straightforwardly obtained by retaining higher S's. (The natural truncation for strong repulsive cases is more complicated and is discussed in ref. 20.) A significant advantage of this theory relative to the Green's function formulation is the fact that the two-body correlations may be expressed in coordinate space in terms of

$$S^{(2)}_{\nu_1\nu_2}(\vec{x}_1,\vec{x}_2) \quad ,$$

a function of two continuous spatial variables and two discrete hole labels, in contrast to the two-particle Green's function containing four spatial variables.

2.3 Limitations of the TDHF Initial Value Problem

One salient limitation of the TDHF approximation is the treatment of two-body correlations. Although in the static case, the strict HF approximation with the bare nuclear potential is rendered totally unphysical by the omission of two-particle two-hole amplitudes, inclusion of short-range correlations via the G-matrix sum of ladder diagrams or some other similar effective interaction yields a very physical and useful mean-field theory. This crucial class of two-particle two-hole contributions associated with the repulsive case is included approximately in the time-dependent case by using in the

time-dependent problem the density-dependent effective interaction derived for ground states. Thus, the time evolution of the two-body correlation function is completely neglected and presumably becomes a serious error in high energy collisions.

A second salient limitation of the TDHF initial value problem concerns its semiclassical aspects. One is forced to construct an initial condition appropriate to the physical problem of interest and consistent with the subsequent approximations in the mean field evolution. In the scattering problem, one localizes the initial nuclei in velocity and impact parameter and seeks to interpret the subsequent density matrix as that arising from wave packets suitably defined for the scattering problem. However, since many inequivalent wave functions can have the same one-body density matrix, it is clear that substantial conceptual problems exist. At a more practical level, the problem of specifying appropriate initial conditions is quite evident if one tries to construct approximations to quantum eigenstates of large amplitude collective vibrations or to calculate the lifetimes for tunneling decay of a fissionable nucleus. In the former case, no initial condition appears natural, and in the latter case, the obvious candidate is the deformed HF stationary state which has the unphysical property of having at time-independent one-body density matrix when evolved with the TDHF equations.

2.4 Treatment of Two Body Correlations

Some insight into the role of two-body correlations may be obtained from the exactly solvable two-level Lipkin model[12] specified by the Hamiltonian

$$H = \frac{\varepsilon}{2} \sum_{\substack{p \\ \sigma=\pm 1}} \sigma a^{+}_{p\sigma} a_{p\sigma} + \frac{V}{2} \sum_{\substack{pp' \\ \sigma=\pm 1}} a^{+}_{p\sigma}\, a^{+}_{p'\sigma}\, a_{p'-\sigma}\, a_{p-\sigma} \tag{11}$$

The ground state energy for a 14 particle system as a function of interaction strength V is shown in Fig. 9 first for the HF approximation and then including the two-particle two-hole amplitude S_2 in the coupled cluster theory.[20] Although the effect of two-body correlations is less drastic than for hand-core nuclear potentials, one still observes a dramatic improvement in the ground state energy.

To emphasize the fact that few-body operators are well described while the many-body wave function is meaningless, the operator

$$J_Z = \frac{1}{2} \sum_p (a^+_{p+} a_{p+} - a^+_{p-} a_{p+})$$

which counts the number of particles in the upper state minus the number in the lower state is considered in Fig. 10. Since the Lipkin Hamiltonian only moves pairs of particles, projection of the ground state wave function (evolved adiabatically from the non-interacting ground state) onto states of specified number in each level must yield the odd-even alternation shown by the solid line in Fig. 10. Since no low-order approximation has any information concerning such 14-body correlations, the HF and S_2 approximations display no such alternation but yield quite adequate approximations to $\langle J_z \rangle$ and $\langle J_z^2 \rangle$.

Finally, application of the time-dependent coupled cluster approximation to two 14-particle Lipkin systems which begin in their respective ground states and then form a 28-particle interacting system for time T yields the results shown in Fig. 11. Again, one observes that expectation values of the two-body operators H and

$$J_x^2 = \sum_p \left\{ \left[a^+_{p+} a_{p-} + a^+_{p-} a_{p+} \right] \right\}^2$$

are systematically improved by the inclusion of S_2. Hence, we conclude that, in general, evolution of S_2 is required to obtain reliable expectation values of two-body operators. Thus it is not surprising that although mean fragment masses are well reproduced in TDHF, the dispersion in particle number is systematically in error. Although the Lipkin model is quite oversimplified, one should note that numerical solution of the coordinate-space coupled cluster equations in ref. 20 is feasible for repulsive core potentials in one spatial dimension, and would shed considerable light on the role of two-body correlation corrections to the mean field theory.

2.5 Derivation of a Quantum Mean-Field Theory Using Functional Integrals

corrections to the mean field theory.

2.5 *Derivation of a Quantum Mean-Field Theory Using Functional Integrals*

Stimulated by developments in quantum field theory in which systematic expansions are developed about the solution to the corresponding classical field equations, significant progress has been made recently in formulating the quantum many-body problem in terms of an expansion about solutions to appropriate mean field equations.[23-25] In contrast to the TDHF initial value problem, the theory is conceptually unambiguous since one applies approximations directly to exact expressions for quantum observables.

The essential steps in the method are as follows. First, one selects a few-body operator corresponding to a physical observable of interest and then one expresses its expectation value in terms of the evolution operator. For example, to calculate the bound state spectrum and the expectation value of any few-body operator σ in any bound state, one may evaluate the poles and residues of the following expression:

$$-i \int dT\, e^{iET}\, tr\, \sigma\, e^{-iHT} = \sum_n \frac{\langle n|\sigma|n\rangle}{E-E_n+iz} \tag{12}$$

Next, one utilizes an appropriate functional integral representation for the many-body evolution operator. One particularly simple choice is the Hubbard-Stratonovich transformation used in ref. 23

$$T e^{-\frac{i}{2}\int dx dx' dt\, \hat{\rho}(x,t)\, \sigma(x-x')\hat{\rho}(x't)} = \int D[\sigma]\, e^{\frac{i}{2}\int \sigma v \sigma}\, T e^{-i\int \sigma v \hat{\rho}} \tag{13}$$

which replaces the evolution operator corresponding to a Hamiltonian containing two-body interactions by an integral over an infinite set of evolution operators containing only one-body operators. A second alternative breaks the evolution into very small time steps

between each of which an overcomplete set of Slater determinants is inserted[25)]

$$\langle\Psi_f|e^{-iHT}|\Psi_i\rangle = \langle\Psi_f|\cdots e^{-iH\Delta T}\int du(z)\ |\Psi(z)\rangle\langle\Psi(z)|e^{-iH\Delta T}\ |\Psi_i\rangle \qquad (14)$$

The theory is rendered manageable by virtue of a simple choice of the measure $du(z)$ which efficiently handles the overcompleteness. A third alternative is to simply use Grassman variables as in field theory[24)], so that the trace of the exponential of the action becomes

$$\mathrm{tr}\ e^{iS} = \int D[Z^*,Z]\ e^{i\left[\int Z^*\left(i\frac{\partial}{\partial t}-T\right)Z - \frac{1}{2}\int Z^*Z^*v\,ZZ\right]} \qquad (15)$$

Finally, for any of these functional integral representations, application of the stationary-phase approximation (SPA) yields TDHF equations plus a systematic hierarchy of corrections.

The essence of the program is exemplified by applying it to the trivial problem of one-dimensional quantum mechanics in the potential shown in Fig. 12, for which case we may write [26)]

$$\mathrm{Tr}\ \frac{1}{H-E} = i\int dT\ e^{iET}\int dq\ \langle q|e^{-iHT}\ |q\rangle$$

$$= i\int_0^\infty dT\ e^{iET}\int dq\int D[q(t)]\ e^{iS[q(t)]}\Big|_{q(t)=q(0)=q} \qquad (16)$$

where $S[q(t)]$ in the Feynman path integral denotes the classical action. Application of the SPA to $\int D[q(t)]$ requires that $q(t)$ must satisfy the classical equation of motion

$$m \frac{d^2}{dt^2} q = -\nabla V \tag{17}$$

and application of the SPA to $\int dq$ requires that the momentum at time T equal that at time 0. Thus, we obtain

$$\mathrm{Tr} \frac{1}{H-E} = i \int_0^\infty dT \sum_{q_{c\ell}} e^{i(ET+S(T))} \equiv i \int dT \sum_{q_{c\ell}} e^{iW(t)} \tag{18}$$

where $S(T)$ is the action for a periodic solution to the classical equation of motion and the sum $\sum_{q_{c\ell}}$ over all such periodic classical solutions.

Finally, the SPA is applied to the time integral in eq. (18), giving rise to both real and complex stationary values of the period. Real periods simply correspond to multiples of the fundamental periods for classical oscillations around minima (a) and (c) in Fig. 12 such that the classical energy equals E. The period and contribution to the reduced action $W(T)$ of eq. (18) for periodic solutions in region a (and similarly for region c) are

$$T_a = 2 \int dq \sqrt{\frac{m}{2(E-V(q)}} \tag{19}$$

and

$$W_a = \oint p\dot{q}\, dt = 2 \int \sqrt{2m(E-V(q))}\, dq \tag{20}$$

The meaning of classical solutions for imaginary time is most evident if one simply replaces it by τ in the equation of motion. The two resulting factors of i in eq. (17) are then equivalent to reversing the sign of $V(q)$. As sketched in Fig. 12, this has the effect of interchanging classically allowed and forbidden regions, so one now has periodic solutions in region b with imaginary period and reduced action

$$i\,T_b = \bar{T}_b = 2\int dq \sqrt{\frac{m}{2(V(q)-E)}} \tag{21}$$

and

$$iW_2(E) \equiv \bar{W}_2(E) = 2\int \sqrt{2m(V(q)-E)}\,dq \tag{22}$$

Combining all integral numbers of periods in the three regions thus yields an infinite sequence of stationary points $T_{\ell mn} = \ell T_a + mT_c - n\bar{T}_b$ and the corresponding sum over classical periodic trajectories in eq. (18) yields multiple geommetric series which sum to

$$\mathrm{Tr}\,\frac{1}{H-E} = \frac{e^{iW_a} + e^{-\bar{W}_b} + e^{iW_c} - 2e^{i(W_a+W_c)}}{\left(1-e^{iW_a}\right)\left(1-e^{iW_c}\right) - e^{\bar{W}_b}} \tag{23}$$

For the case of a single well, in which case regions (b) and (c) don't exist, this yields poles at energies E_n such that

$$W_1(E_n) = \int p\,dq = 2n\,\pi \tag{24}$$

Equation (24) differs from the usual Bohr-Sommerfeld quantization condition $(2n+1)\pi$ only because we have neglected phase factors arising from quadratic corrections to the SCA. In the case of spontaneous decay of a quasi-stationary state, region (c) is elongated to

extend throughout an arbitrarily large normalization box, and one observes that W_c then yields a vanishing contribution to the smoothed level density[27]

$$P_\gamma \equiv \frac{1}{\pi} \operatorname{Im} \operatorname{Tr} \frac{1}{E - H + i\gamma} \propto \left[\left(\frac{e^{-\bar{W}_b}}{2} \right)^2 + \left(\sin \frac{W_a}{2} \right)^2 \right]^{-1} \tag{25}$$

The level density, eq. (25), exhibits quasi-stationary states with energies given by eq. (24) and widths

$$\Gamma_n = 2 \left(\frac{\partial W_a}{\partial E} \right) e^{-\bar{W}_b(E_n)} = 2\, T_a\, e^{-\bar{W}_b(E_N)} \tag{26}$$

which agree with the familiar WKB result.

Straightforward application of the same program to the many-body problem results in application of the SPA to the T and σ integrals in an expression of the form

$$\int dT\, e^{iET}\, \operatorname{tr} e^{-iHT} = \int dT\, e^{iET} \int D[\sigma]\, e^{-S[\sigma]} \tag{27}$$

and yields three distinct classes of solutions.

Time-independent solutions to the SPA equations reproduce familiar HF theory. The quadratic corrections to SPA produce the RPA ground state correlations, and the systematic evaluation of higher corrections simply generates standard perturbation theory. Aside from providing a terse and elegant derivation of perturbation theory, this functional integral approach has the additional advantage of dealing efficiently with constraints, such as those arising in gauge theories.[28]

A second class comprises time-dependent solutions with real period which correspond to eigenfunctions of large-amplitude collective motion. A set of N single-particle wave functions obey the following eigenvalue equation

$$\left[-i \frac{\partial}{\partial t} + K + \operatorname{tr}_2 v\sigma \right] \phi_i(x,t) = \alpha_i \phi_i(x,t) \tag{28}$$

subject to the periodic boundary condition

$$\phi_i\left(x, \frac{T}{2}\right) = \phi_i\left(x, -\frac{T}{2}\right) \tag{29}$$

where the self-consistent mean field satisfies

$$\sigma(x,x',t) = \sum_i \phi_i^*(x',t)\,\phi_i(x,t) \tag{30}$$

and the allowed values of the period are specified by the quantization condition

$$\int dx \int_{-T/2}^{T/2} dt\; \phi^*(x,t)\, i\,\frac{\partial}{\partial t}\,\phi(x,t) = n\,2\pi \tag{31}$$

Clearly the non-linear differential eqs. (28-30) in four space-time dimensions have the same general structure as the static Hartree equations in three space dimensions, and they may be solved by the usual iterative procedure. Application of this method to the ground state multiplet of the spectrum of the Lipkin model yields the results shown in Fig. 13. Further discussion of large amplitude collective motion using this general approach may be found in ref. 24.

The third class of solutions is made up of time-dependent solutions with imaginary period corresponding to tunneling phenomena in classically forbidden domains. In this case, the single-particle equations (28) are replaced by

$$\left[\frac{\partial}{\partial t} + K + \mathrm{tr}\,\sigma v\right]\phi_i(x,t) = \alpha_i\phi_i(x,t) \tag{32}$$

with the same periodic boundary condition (29) and the self-consistent mean field

$$\sigma(x,x',t) = \sum_i \phi_i(x',-t)\phi_i(x,t) \tag{33}$$

Of particular physical interest are solutions which in the limit as $\pm T/2 \to \pm \infty$ approach the HF stationary local minimum for a fissioning nucleus and evolve near $T \sim 0$ toward the entrance to the classically allowed domain near the scission point for two fission fragments. Such solutions will be denoted "bounces," following Coleman, and bear great formal similarity to the "pseudoparticles" and "instantons"[31] investigated extensively in field theory. Whereas the Euclidean solutions arising in field theory have trivial spatial dependence, being either constant or spherically symmetric in space-time, the nontrivial spatial dependence of the present "bounce" solutions is crucial to the physics and precludes analytic solution even for schematic models. Furthermore, for a nucleus possessing many decay channels such as symmetric fission, asymmetric fission, alpha, proton, or neutron decay, there will exist several distinct well-separated bounces, and the analog of the width Γ in eq. (26) is the sum of partial widths:

$$\Gamma = \sum_m \Gamma^{(m)} \tag{34}$$

where each partial width is calculated from the action determined for the bounce solution for the appropriate channel

$$\Gamma^{(m)} = \nu \, T_m \, e^{-\int dx \int_{-T/2}^{T/2} d\tau \, \phi(x,-\tau) \frac{\partial}{\partial \tau} \phi(x,\tau)} \tag{35}$$

To make these bounce solutions more concrete, it is useful to consider a saturating model system of nuclei in one spatial dimension interacting with an effective interaction of the Skyrme form.[24] The analog of the Coulomb force is adjusted such that a 16-particle system is unstable with respect to fission into two 8-particle daughters which are in turn stable with respect to further decay into 4-particle granddaughters. The constrained HF energy as a function of $\langle x^2 \rangle$ for the 16-particle system is shown in Fig. 14, and displays the expected form of a fission barrier. The self-consistent single-particle solutions to eqs. (32), assuming spin-isospin degeneracy 4, are shown in Fig. 15 at the two turning points, $\tau = \pm T/2$ and $\tau = 0$. As expected, the determinant of these wave functions corresponds to the 16-particle HF static solution at $\tau = \pm T/2$ and closely approximates the product of two 8-particle determinants for nearly-separated fragments at $\tau = 0$. The corresponding density, $\sigma(x,t)$ is shown in Fig. 16 for successive times between $\tau^2 = -T/2$ and $\tau = 0$.

Solution of eqs. (32) in four space-time dimensions is obviously computationally more cumbersome, but has been accomplished for a range of nuclei up to $A = 32$. In these calculations, the proton charge has been increased to obtain appropriate values of the fissility, and preliminary results for the fission of ^{8}Be are shown in Fig. 17. Although spurious cm motion problems prevent quantitative comparison of this particular calculation with experiment, this result does demonstrate the feasibility of obtaining bounce solutions with the appropriate properties and shows that all the relevant shape degrees of freedom really are incorporated in this self-consistent theory.

Clearly, many other applications of quantum mean-field approximations arising from such functional integral expressions are possible. One should not only be able to understand shell effects and the competition between symmetric and asymmetric channels in spontaneous fission, but also be able to address compound nucleus decay. Reaction theory poses many important and challenging problems. Whereas it is relatively straightforward to write down tractable mean field expressions for S-matrix elements, we have emphasized above that there is no reason for believing that a mean field theory is really capable of describing the overlap of two many-body wave functions. The key to a meaningful reaction theor

believe, is finding an appropriate functional integral expression for relevant expectation values of few-body operators, such as mean fragment charge, mass, or excitation energy, which yields numerically tractable mean-field equations. In contrast to the TDHF initial value problem, which describes the most probable outcome, such functional integral expressions for specific observables can address specific components of interest, even those which are exponentially small relative to the most probable component. This, then, is the natural language to address such diverse and important questions as superheavy nucleus formation in heavy ion collisions, and tunneling phenomena in light-ion collisions associated with quasi-molecular states and the resonance behavior in such systems as ^{24}Mg. Finally, application of analogous techniques to field theories such as the two-dimensional σ model offers one the only available means to investigate the dynamics of forming abnormal states in appropriate finite geometry.[32]

4. Application to Pion Condensation in Finite Systems

To focus many of the general ideas associated with my discussions of the time-dependent mean field theory on a concrete problem relevant to a somewhat extreme state of nuclear systems, I will conclude my talk with some remarks relating to the observation of pion condensation in finite systems. For simplicity, I will consider the static limit in which pion propagators are reduced to the static limit, and pions thus enter only through a renormalized nuclear interaction containing a one-pion exchange potential. At the onset of condensation, $\omega = 0$, rendering the static reduction exact, and the approximation should remain valid for finite ω much less than the pion mass μ. For the present discussion, it is sufficient to consider an interaction of the Fermi liquid form augmented with an explicit OPEP term, which has the following spin-isospin components:

$$V(q) = g' \sigma_1\cdot\sigma_2\ \tau_1\cdot\tau_2 - \frac{4\pi f^2}{\mu^2}\frac{1}{q^2+\mu^2}\ \sigma_1\cdot q\ \sigma_2\cdot q\ \tau_1\cdot\tau_2 \qquad (36)$$

In the time-dependent mean-field framework, the natural quantity of interest is the RPA propagator which simply describes the TDHF evolution of a system for infinitesimal amplitude excitations and thus contains all the relevant information about modes having the quantum numbers of the pion. In infinite matter, the RPA propagator contains the factor:

$$\Pi \propto \left[1 - \left(g' - \frac{4\pi f^2}{\mu^2} \frac{q^2}{\mu^2+q^2} \right) 4 \Pi_0(q) \right]^{-1} \tag{37}$$

where the Lindhardt function is defined

$$\Pi_0(q, k_F) = \sum_{\vec{p}} \frac{\theta(|\vec{p}+\vec{q}| - k_F)\ \theta(k_F - |p|)}{\epsilon_{|\vec{p}+\vec{q}|} - \epsilon_{|\vec{p}|}} \tag{38}$$

4.1 Optimal Experiments for Precursor Phenomena

From the perspective of mean-field theory, there is no question as to how to go about looking for soft spin modes in a pot of liquid helium. One simply measures the response function which specifies the spin response at some space-time point to an arbitrarily weak spin excitation at some other point. As is well known, inelastic electron scattering measures precisely the response function of a finite nucleus[34], so that one may directly study the finite nucleus analog of the polarization propagator in eq. (37).

Measuring the response function through inelastic electron scattering has the following distinct advantages relative to the popular but ambiguous experiments in which unnatural parity states are excited in ^{12}C by protons or electrons. In the first place,

Fig. 18 Density and divergence of spin-isospin density for head on $^{15}N = {}^{15}N$ collision at a cm energy of 20 MeV/A.

the linear response function may be consistently approximated in the mean-field theory. In contrast, the matrix element $\langle\psi_f|M|\psi_i\rangle$ irrevocably tangles up structure from shell model calculations of $|\psi_f\rangle$ and $|\psi_i\rangle$ with that of the operator M which is supposed to contain a signature of the soft pion mode. Secondly, a Rosenbluth separation of longitudinal and transverse form factors affords the opportunity of comparing in a single experiment the response to the charge coupling in the spin-independent channels and the magnetic moment coupling to the spin-dependent channels. Since the soft pion-like modes occur only in the spin-dependent channels, it is clear that the ratio of the two response functions affords an unusually high degree of model independence. Finally, it is useful to note that sophisticated RPA codes already exist[35], and that experiments to separate longitudinal and transverse form factors are presently underway at MIT and Saclay.

4.2 Pion Condensation in Heavy Ion Reactions

The conventional approach to pion condensation in heavy ion reactions is to calculate first the equation of state of equilibrated nuclear matter, including the phase transition from the normal to the condensed phase, and then assume that hydrodynamics governs the dynamics of the nuclear collision. Such an approximation which assumes equilibration on a scale small relative to the scale of spatial variations of the system and allows collective phenomena to enter only through the equation of state may be fine for the collisions of neutron stars, but in view of the earlier discussion of longitudinal momentum equilibration lengths, is clearly inadequate for collisions of finite nuclei. Furthermore, despite claims to the contrary, critical scattering in the presence of a pion condensate is not particularly effective in diminishing the longitudinal equilibration length, since the optimal condensate direction is perpendicular to the beam direction and critical scattering thus involves only momentum transfers of magnitude equal to the critical momentum in the transverse direction. In effect, the condensate thus occurs in the worst possible direction for longitudinal momentum equilibation.

In contrast, in the mean-field theory, the mean field consistently governs evolution of both the bulk matter and the growth of spin isospin instabilities. A neutral pion condensate in this language corresponds to coherent spin-isospin density fluctuations in which an alternating layer structure arises with layers of excess spin up protons and spin down neutrons alternating with layers of excess spin up neutrons and spin down protons, giving rise to a non-zero expectation value of the source term of the pion field $\nabla \cdot \langle \vec{\sigma} \tau \rangle$. As two colliding ions first interpenetrate, the one-body density matrix in the overlapping region corresponds approximately to two separated Fermi spheres centered at $\pm P/2$, where P represents the relative momentum. The initial growth of a spin-isospin instability is thus well described by the RPA propagator, eq. (3.), where the Lindhardt function is now evaluated for two separated Fermi spheres. The contrast between this mean field result and the conventional assumption of equilibrated matter is thus quite dramatic. Whereas the driving term for condensation in the case of a single Fermi sphere of radius k_f is $\Pi_0(q,k_f)$, the driving term for the two interpenetiating Fermi gases corresponding to the same total density is $2\,\Pi_0(q,\, 2^{-1/3}\, k_f)$ if $\frac{P}{2} > k_f$ and the condensate occurs perpendicular to the beam As a result, for a system in which condensation only occurs at three times nuclear matter density in equilibrated matter, the same interaction will yield condensation for two interpenetrating gasses at a total density of only about one and a half times nuclear matter density. This effect immensely increases the chance that a spin-isospin instability actually does occur in high energy heavy ion collisions.

A first attempt at calculating the buildup of spin-isospin instabilities in the mean-field approximation[37] is shown in Fig. 18 for a head-on collision of ^{15}N on ^{15}N. Density distributions as a function of r and z are shown at successive times in the left-hand plots and the pion source term $\nabla \cdot \langle \sigma \tau \rangle$ is displayed in the right-hand plots.

Since the initial spins were selected anti-aligned, if there were no non-linear growth of the mode, the source term would vanish at maximum overlap ($t = 1.125 \times 10^{-22}$ sec). One observes, however, that during maximum overlap, the spin-isospin fluctuation is in fact larger than in either of the original nuclei, clearly indicating growth of the mode. Unfortunately, as soon as this very small system begins to separate, the effect quickly dies away. There is considerable reason to expect that for larger systems, such as Pb + Pb or $^{238}U + ^{238}U$, the larger regions of overlap and longer overlap times would give rise to much larger amplitude fluctuations. In fact, my present belief is that spin-isospin instabilities actually do occur during collisions of heavy nuclei at cm energies of the order of 20 MeV/A. The most troubling worry, however, is that although such interesting instabilities actually occur in nature, there may well be no practical experiment which results in an unambiguous signature of their existence.

Conclusion

I hope to have demonstrated in this survey that the time-dependent mean-field theory is a versatile and powerful approach to the nuclear many-body problem. For many applications, it is the simplest theory which has any chance of incorporating the essential physics of the problem. It may well be computationally cumbersome, but the cost of relevant calculations is still very small on the scale of the expense of the corresponding experiments. Finally, I hope to have shown that it provides a useful framework to think about extreme, as well as ordinary, states of nuclear systems.

REFERENCES

1) J. J. de Swart, Proceedings of this conference.

2) M. Sobel, P. Siemens, J. Bondorf, and H. A. Bethe, Nucl. Phys. A251, 502 (1975).

3) J. W. Negele and D. Vavtherin, Phys. Rev. C5, 1472 (1972).

4) J. W. Negele, Proceedings of Conf. on Nucleon-Nucleon Interactions, Vancouver (1977 B. D. Day, Rev. Mod. Phys. 50, 495 (1978); V. R. Pandharipande & R. B. Wiringa, Rev. Mod. Phys. 51, 821 (1979).

5) J. W. Negele, Proc. NATO/NSF Summer School on Theoretical Methods in Medium Energy and Heavy Ion Physics, Madison, WI, Plenum Press (1978).

6) J. W. Negele, Proc. of International Conference on Effective Interactions and Operators in Nuclei, ed. B. R. Barrett, Springer-Verlag (1975).

7) Proceedings of Saclay Workshop on the Time Dependent Hartree Fock Method, Saclay (1979).

8) S. E. Koonin, in ref. 7.

9) J. L. Friar, J. Heisenberg, and J. W. Negele, Proc. Workshop in Intermediate Energy Electromagnetic Interactions with Nuclei, M.I.T., A. M. Bernstein ed. (1977).

10) D. Gogny, Proceedings International Conf. on Nuclear Physics with Electromagnetic Interactions, Mainz, H. Arenhövel and D. Drechsel ed, Springer Verlag, Berlin (1979).

11) J. W. Negele and G. A. Rinker, Phys. Rev. C 15, 1499 (1977).

12) C. Creswell, Ph.D. dissertation, Massachusetts Institute of Technology (1979).

13) G. F. Bertsch and S. F. Tsai, Phys. Repts. 18, 125 (1975).

14) P. Bouche, B. Grammaticos, and S. E. Koonin, Phys. Rev. C 17, 1700 (1978).

15) K.T.R. Davies, V. Maruhn-Rezwani, S. E. Koonin, and J. W. Negele, Phys. Rev. Lett. 41, 632 (1978).

16) A. K. Kerman and S. E. Koonin, Ann. Phys. (N.Y.) 100 332 (1976).

17) P. C. Martin and J. Schwinger, Phys. Rev. 115, 1342 (1959).

18) H. Orland and R Schaeffer, Saclay preprint DPh-T/78/41.

19) C. Y. Wong and H. H. K. Tang, Phys. Rev. Lett. 40, 1070 (1978).
20) P. Hoodbhoy and J. W. Negele, Phys. Rev. C 18, 2380 (1978); 19, 1971 (1979).
21) H. Kümmel, K. H. Lührmann, and J. G. Zabolitzky, Phys. Repts. 36C (1978).
22) H. J. Lipkin, N. Meshkov, and A. J. Glick, Nucl. Phys. 62, 188 (1965).
23) S. Levit, J. W. Negele, Z. Paltiel, M.I.T. Preprint CTP 779, (1979) and contributions to ref. 7; J. W. Negele. 1979 Varenna Lectures.
24) H. Reinhardt, Proceedings of this conference and J. Phys. G5 L91 (1979); C. M. Bender F. Cooper, and G. S. Guralnik, Ann. Phys. 109 165 (1977).
25) J. P. Blaizot and H. Orland, Saclay preprint (1980).
26) S. Levit, J. W. Negele, Z. Paltiel, to be published.
27) R. Balian and C. Block, Annals of Physics (NY) 85, 415 (1979).
28) L. D. Faddeev and V. N. Popov, Phys. Lett. 25B 29 (1967); L. D. Faddeev, Theor. Mat. Fiz. 1, 3(1970), (Theor. Math. Phys. 1, 1 (1970)).
29) S. Coleman, lectures at International School of Subnuclear Physics, Ettore Majorana (1977).
30) A. M. Polyakov, Nucl. Phys. B 121 429 (1977).
31) G. 't Hooft, Phys. Rev. Lett. 37, 8 (1976).
32) D. Campbell, contribution to ref. 7.
33) W. Weise, Proceedings of this conference.
34) S. Fetter and J. D. Walecka, Quantum Theory of Many-Particle Systems, McGraw-Hill, N.Y. (1971).

FIGURE CAPTIONS

Fig. 1 Comparison of Saclay electron scattering cross sections for ^{208}Pb with mean field theory predictions.

Fig. 2 Comparison of theoretical and empirically determined charge densities for ^{208}Pb.

Fig. 3 Mean field predictions of shapes of deformed intrinsic states.

Fig. 4 Comparison of mean-field form factors with subsequent experimental results for the ground state rotational band in ^{238}U.

Fig. 5 Comparison of the mean-field theory predictions with subsequent experimental form factors for the octupole vibrations of ^{238}U.

Fig. 6 Comparison of the RPA prediction and experimentally reconstructed transition density for the first 3^- state in ^{208}Pb.

Fig. 7 Comparison of TDHF and experimental fusion cross sections as a function of laboratory energy.

Fig. 8 Comparison of the energy loss as a function of scattering angle predicted by TDHF and measured experimentally.

Fig. 9 The exact ground state energy E (solid line), deviation from E of the HF energy (short dashes), and deviation from E of the coupled cluster energy including S_2 (long dashes).

Fig. 10 Probability P_M of projecting a component with $2M_J + 14$ particles in the upper state from the exact, HF, and second-order coupled cluster ground state wave functions.

Fig. 11 Excitation energy ΔE and mean value of J_x^2 as a function of interaction time for exact, TDHF, and second-order coupled cluster wave functions.

Fig. 12 Sketch of a double well with two classically allowed regions separated by one classically forbidden region.

Fig. 13 Exact Lipkin spectrum (crosses) compared with the mean-field approximation as a function of $\xi^{-1} = NV/\varepsilon$. The dot-dash curves denote doubly degenerate approximate solutions and the other curves are non-degenerate.

Fig. 14 The constrained energy of a 16-particle model system as a function of $\langle x^2 \rangle$.

Fig. 15 Self consistent single-particle wave functions as a function of x at times $\tau = -T/2$ and $\tau = 0$ for the bounce solution for spontaneous fission of a 16-particle model system.

Fig. 16 The density $\sigma(x,\tau)$ for the same system as in Fig. 15 as a function of x at successive times from $\tau = -T/2$ to $\tau=0$.

Fig. 17 Contour plot of integrated density contours displaying the sequential shapes of ^{8}Be from $\tau = -T/2$ to $\tau = 0$.

Fig. 18 Density and divergence of spin-isospin density for head on $^{15}N = {}^{15}N$ collision at a cm energy of 20 MeV/A.

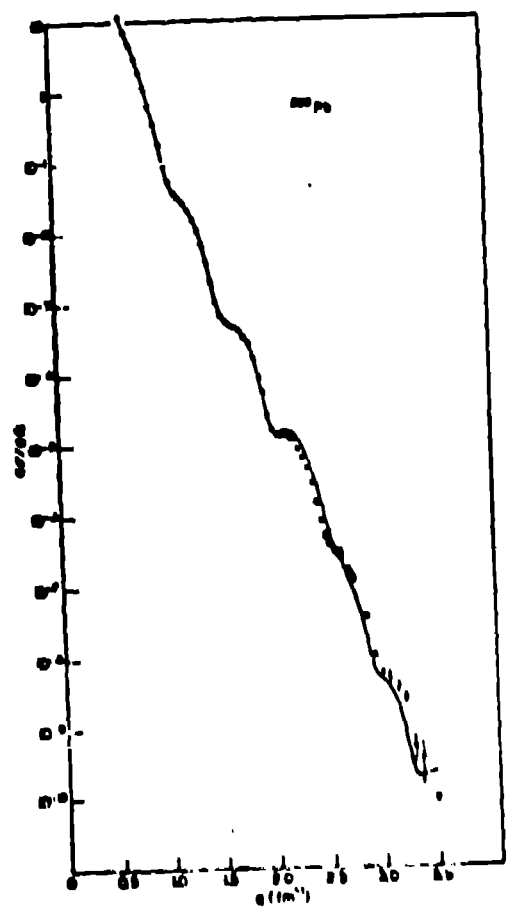

Fig 1

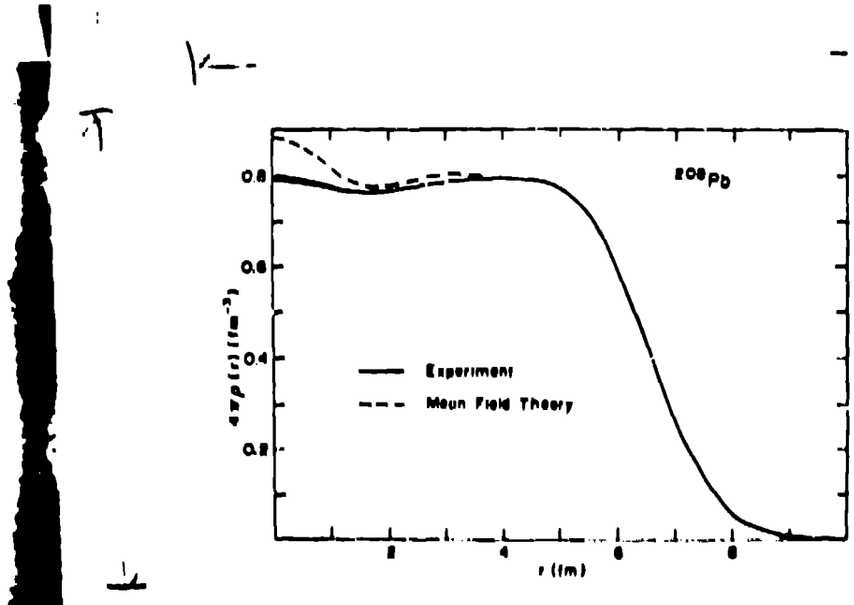
^{208}Pb
Experiment
Mean Field Theory
0.8
0.6
0.4
0.2
2
4
6
8
r (fm)

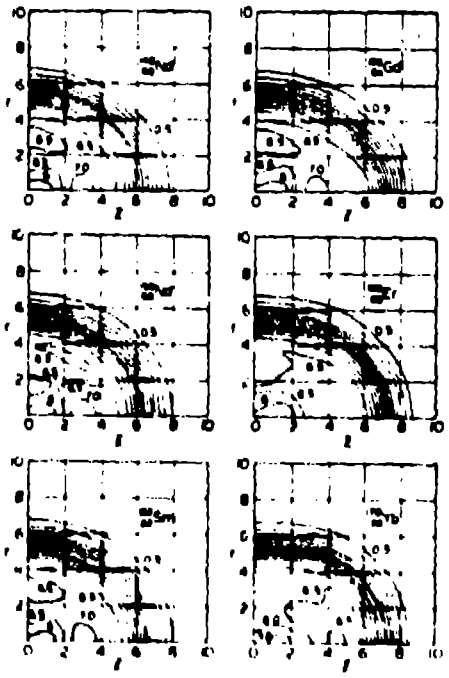

FIG. 3. Contour plots of proton density distributions. The density contours are in increments of 0.004 fm^{-3}, the labels denote the density multiplied by 100, and r and z are in fm.

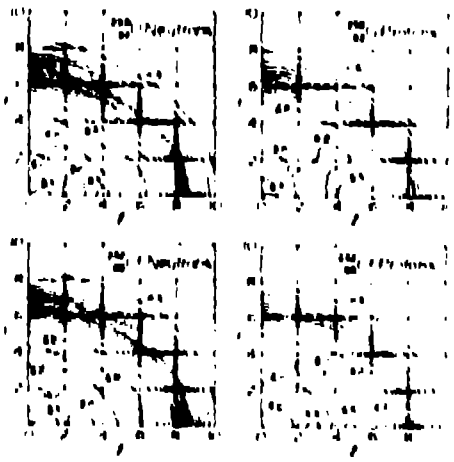

FIG. 4. Proton and neutron density contours for actinides. Scales are as in Fig. 3.

FIG. 6. Elastic ... ^{166}Gd. The notation ... —J", the solid lines ... the error bars denote ...

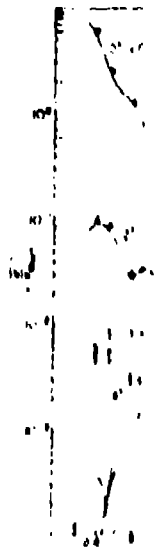

FIG. 5. Elastic ... ^{176}Yb, with the ...

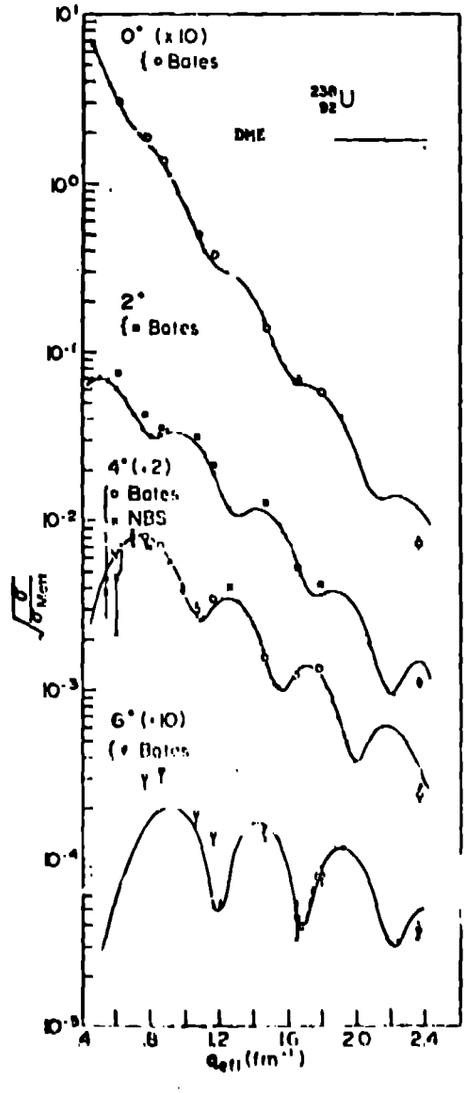
0° (x10)
(∘ Bates
$^{238}_{92}U$
DHE
2°
(▪ Bates
4°(·2)
∘ Bates
▪ NBS
6°(·10)
(▾ Bates
$\sqrt{\frac{\sigma}{\sigma_{Mott}}}$
10^{1}
10^{0}
10^{-1}
10^{-2}
10^{-3}
10^{-4}
10^{-5}
.4
.8
1.2
1.6
2.0
2.4
q_{eff} (fm^{-1})

7.64

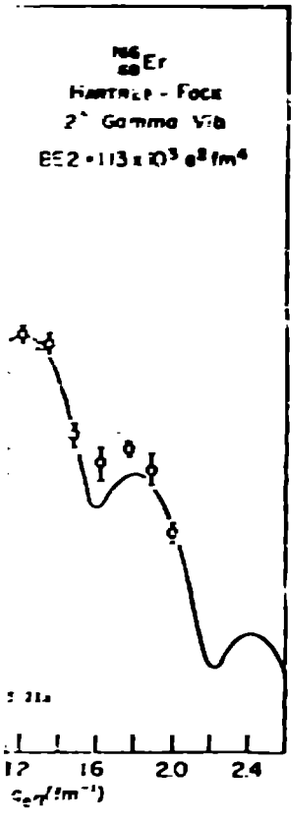
Hartree - Fock
2⁺ Gamma Vib
12
16
20
24

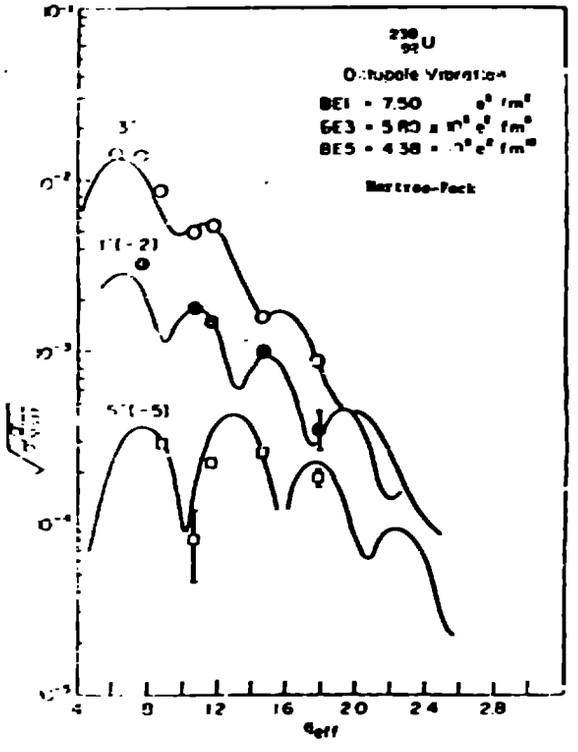
Octupole Vibration
Hartree-Fock
3⁻
1⁻(-2)
5⁻(-5)
4
8
12
16
20
24
28

716 5

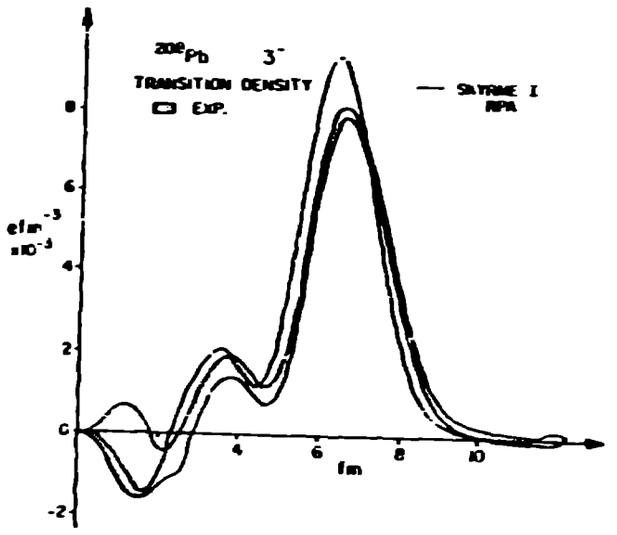
^{208}Pb 3^-
TRANSITION DENSITY
EXP.
— SKYRME I
RPA
efm^{-3}
$\times 10^{-3}$
8
6
4
2
0
-2
4
6
8
10
fm

7i66

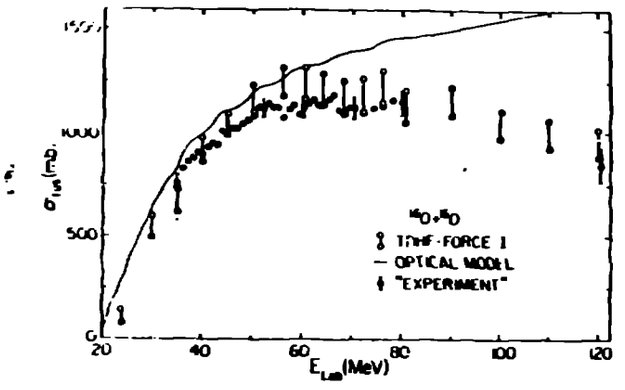
1500
1000
500
0
σ_{tot} (mb)
$^{16}O+^{16}O$
THF-FORCE I
— OPTICAL MODEL
"EXPERIMENT"
20
40
60
80
100
120
E_{Lab}(MeV)

7i67

LIPKIN 2-LEVEL MODEL

$$H = \sum_p \frac{\epsilon}{2}\left(a^\dagger_{\sigma p} a_{\sigma p} - a^\dagger_{-p} a_{-p}\right) + V \sum_{pp'} a^\dagger_{\sigma p} a^\dagger_{-p} a_{-p'} a_{\sigma p'} + a^\dagger_{-p} a^\dagger_{\sigma p} a_{\sigma p'} a_{-p'}$$

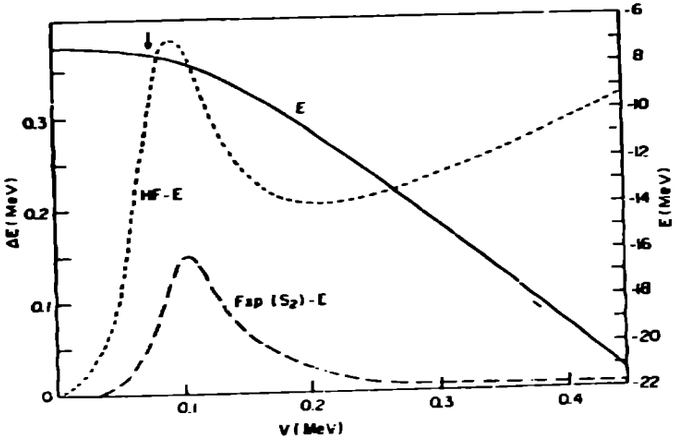

Fig 9

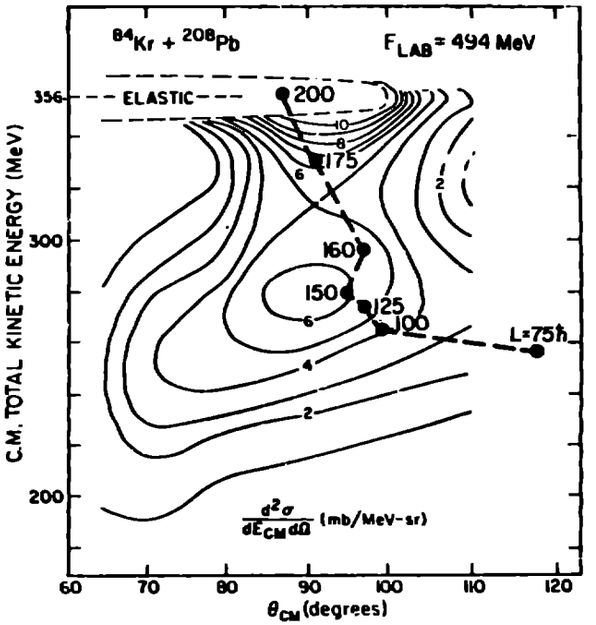

Fig 8

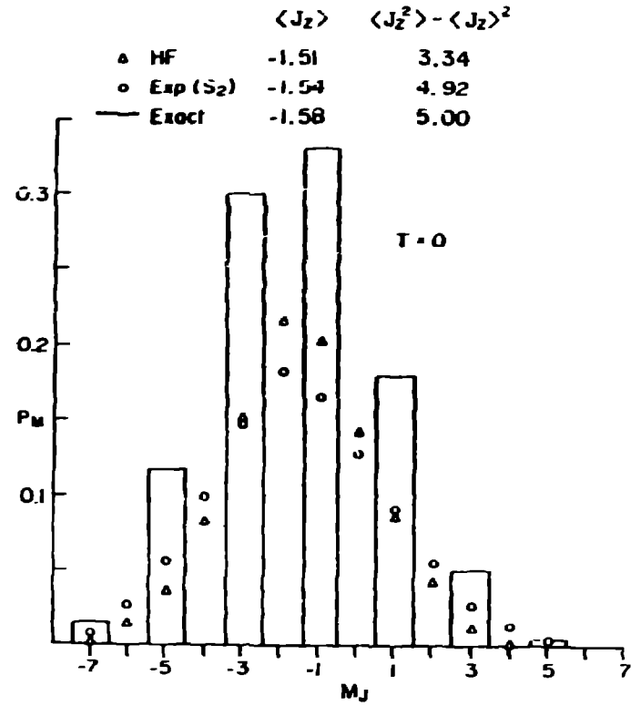
⟨Jz⟩ ⟨Jz²⟩ - ⟨Jz⟩²
HF -1.51 3.34
Exp (Sz) -1.54 4.92
Exact -1.58 5.00
T = 0
0.3
0.2
0.1
PM
-7 -5 -3 -1 1 3 5 7
MJ

Fig 10

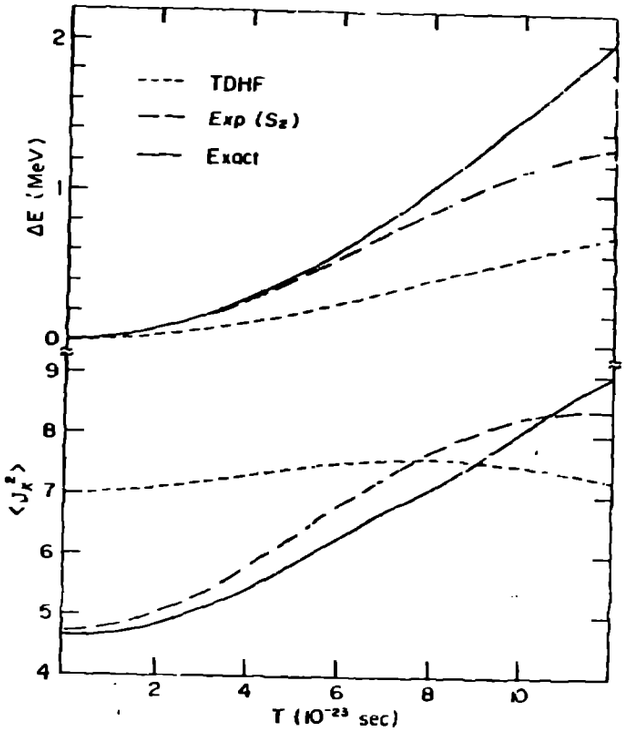
TDHF
Exp (Sz)
Exact
ΔE (MeV)
2
1
0
⟨JK²⟩
9
8
7
6
5
4
2 4 6 8 10
T (10⁻²³ sec)

Fig 11

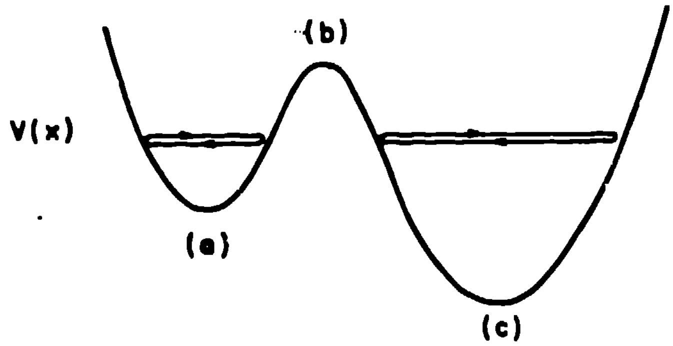
(b)
V(x)
(a)
(c)

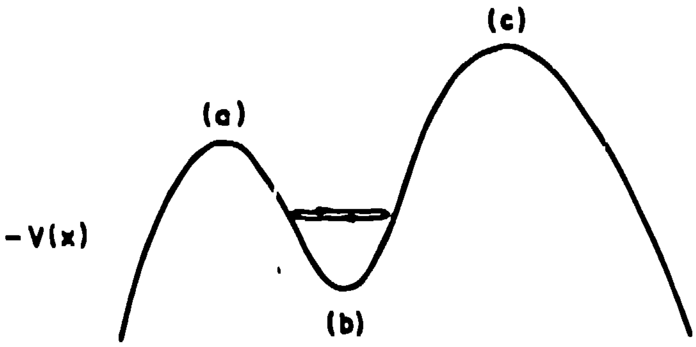
(c)
(a)
-V(x)
(b)

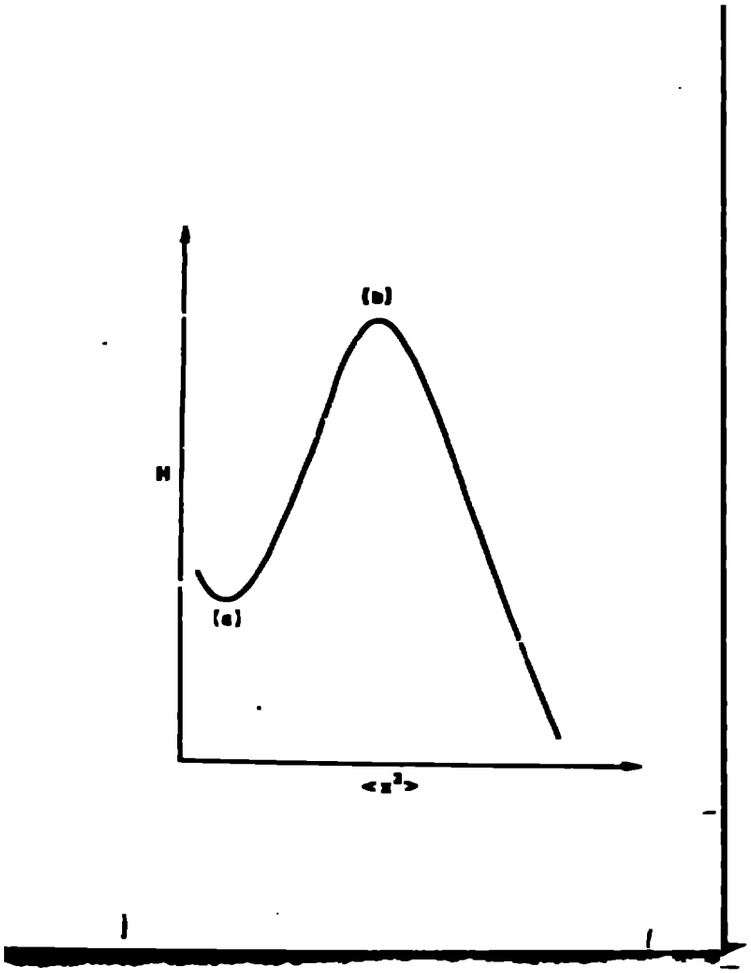

Fig 12

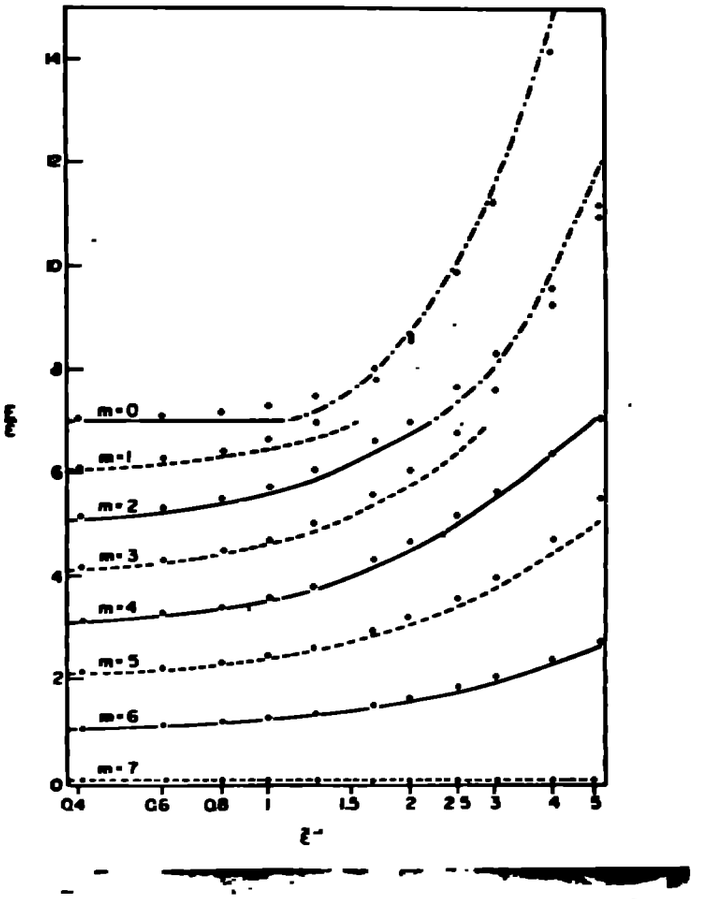

Fig 13

Fig 14

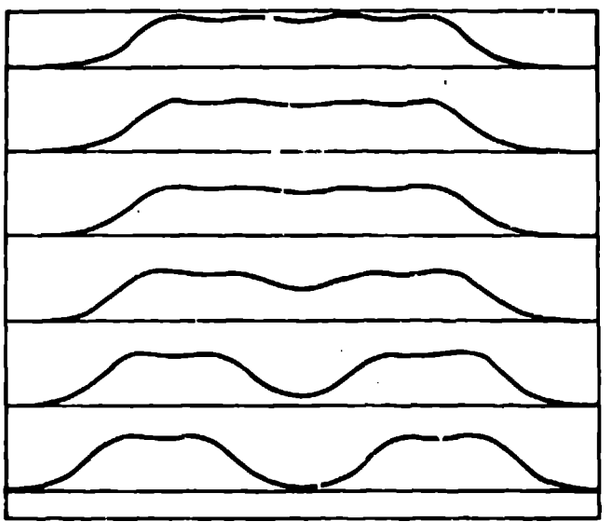

Fig 15

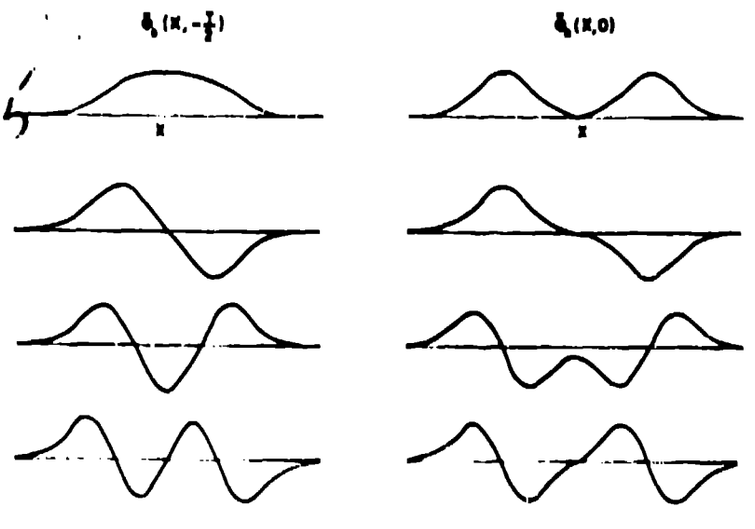

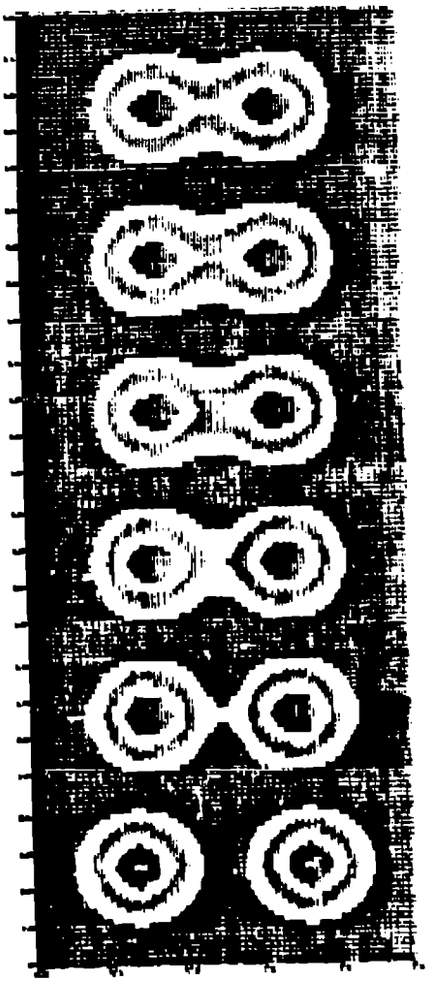

1916 17.

Fig 18